<u>**Supporting Information**</u>

3D Printed Microdroplet Curing: Unravelling the Physics of On-spot Photopolymerization

Vishal Sankar Sivasankar,[1] Harnoor Singh Sachar,[1] Shayandev Sinha,[2] Daniel R. Hines,[3*] and Siddhartha Das[1*]

[1]Department of Mechanical Engineering, University of Maryland, College Park, MD 20742

[2]The Rowland Institute at Harvard, Harvard University, Cambridge, MA 02142

[3]Laboratory for Physical Sciences, 8050 Greenmead Drive, College Park, Maryland 20740, USA

*Email: hines@lps.umd.edu; sidd@umd.edu

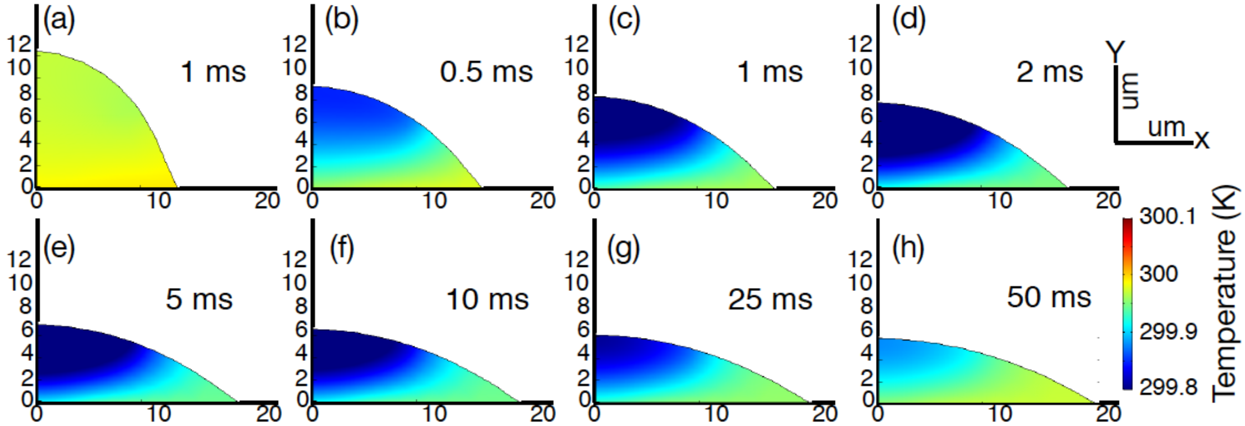

Figure S1(a-h): Temperature distribution within the spreading polymer drop (radius 0.01 mm) at different time instants for case 1 ($\tau_s \ll \tau_p$). Here we have $\tau_s \approx 1.1$ ms and $\tau_p \approx 66$ ms.

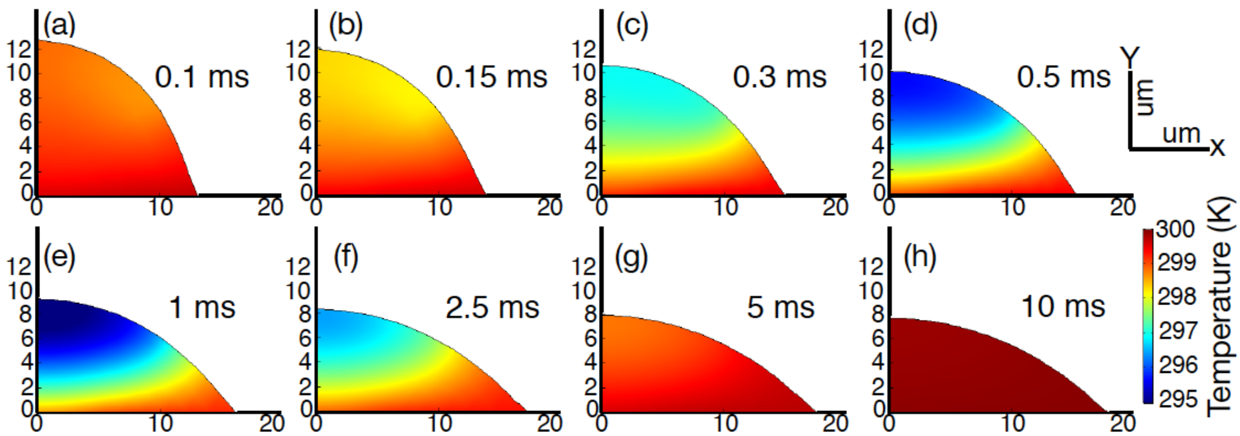

Figure S2(a-h): Temperature distribution within the spreading polymer drop (radius 0.01 mm) at different time instants for case 2 ($\tau_s \sim \tau_p$). Here we have $\tau_s \approx 1.1$ ms and $\tau_p \approx 3.3$ ms.

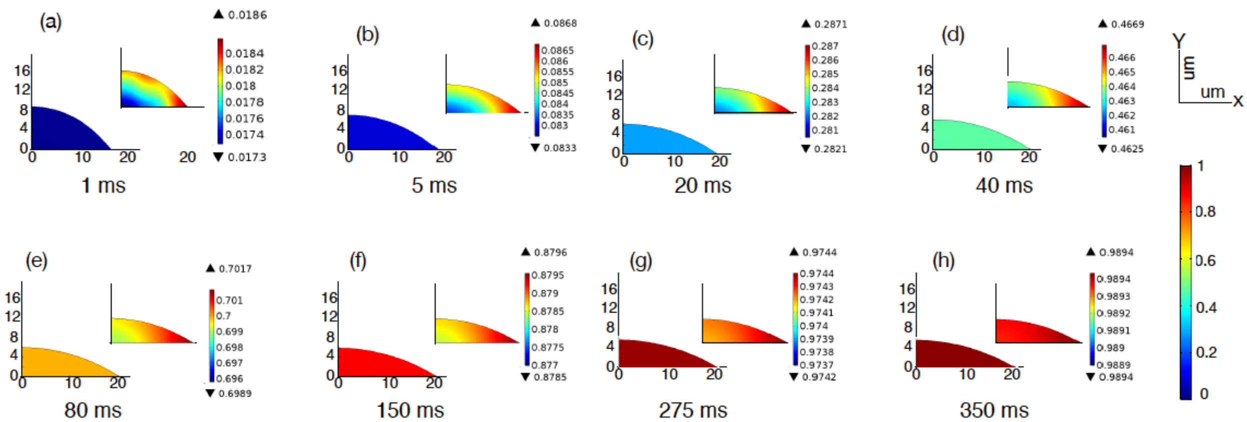

Figure S3(a-h): Curing profiles within the spreading polymer drop (radius 0.01 mm) at different time instants for case 1 ($\tau_s << \tau_p$). Here we have $\tau_s \approx 1.1$ ms and $\tau_p \approx 66$ ms. In the inset of each subfigure, we plot the variation of the curing profile with a much smaller range of the color bar for highlighting the curing profiles (or equivalently, a distribution of the monomer concentration) within the drop itself at a given time instant.

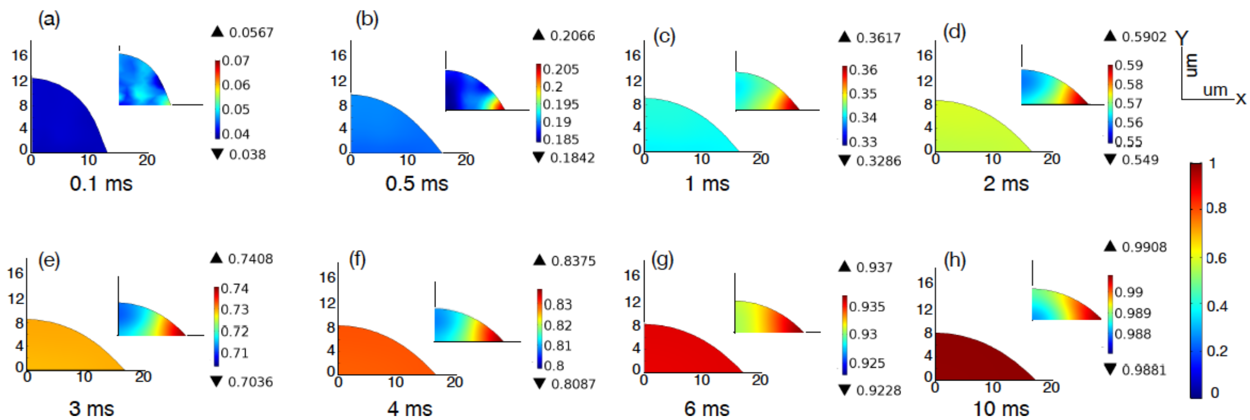

Figure S4(a-h): Curing profiles within the spreading polymer drop (radius 0.01 mm) at different time instants for case 2 ($\tau_s \sim \tau_p$). Here we have $\tau_s \approx 1.1$ ms and $\tau_p \approx 3.3$ ms. In the inset of each subfigure, we plot the variation of the curing profile with a much smaller range of the color bar for highlighting the curing profiles (or equivalently, a distribution of the monomer concentration) within the drop itself at a given time instant.

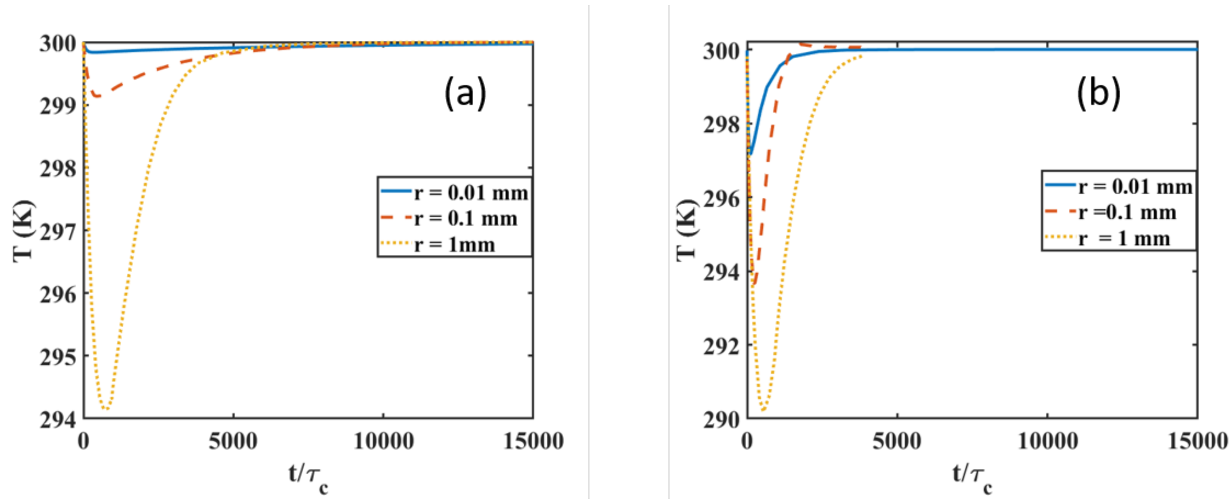

Figure S5: Variation of the average temperature of the drop with t/τ_c for (a) Case 1 and (b) Case 2 for the drops of three different sizes. The different parameters have been summarized in the caption of Fig. 8 of the main paper.

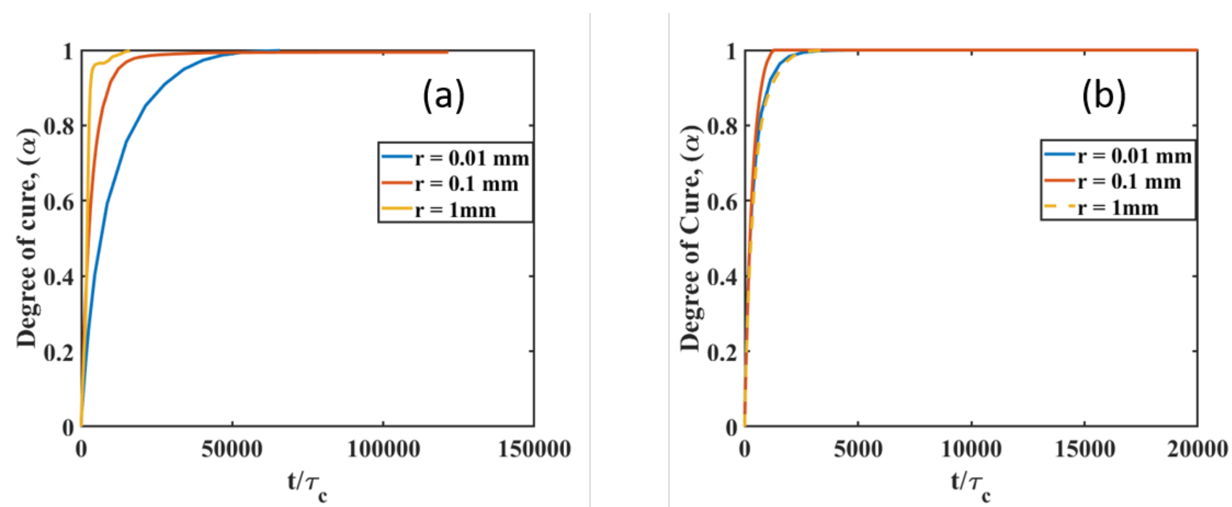

Figure S6: Variation of the average degree of cure for the drop with t/τ_c for (a) Case 1 and (b) Case 2 for the drops of three different sizes. The different parameters have been summarized in the caption of Fig. 8 of the main paper.

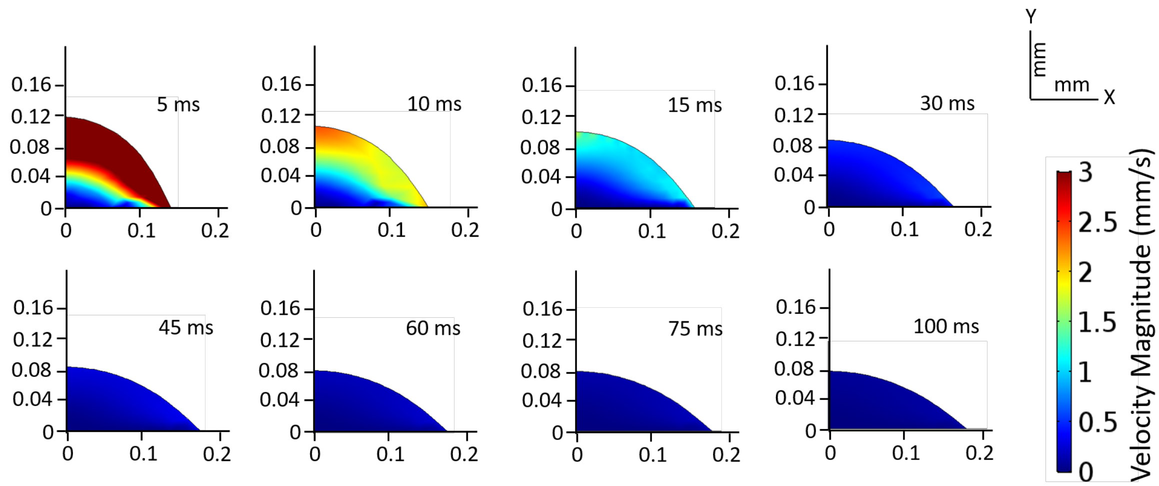

Figure S7: Velocity distribution within the spreading polymer drop at different time instants for case 1 ($\tau_s << \tau_p$) for a drop of radius 0.1 mm. Here we have $\tau_s \approx 10.2$ ms and $\tau_p \approx 660$ ms. Velocity profiles within the air have not been shown for the sake of clarity.

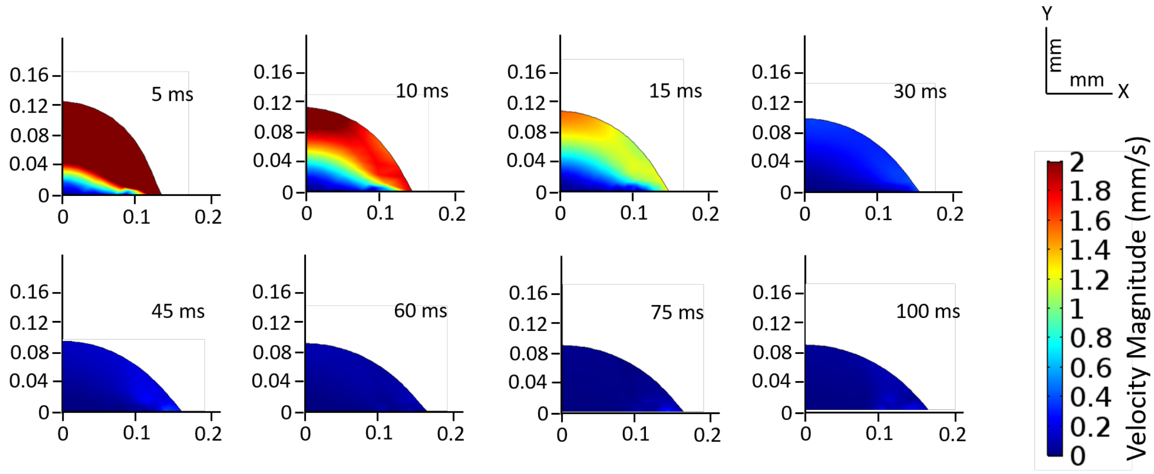

Figure S8: Velocity distribution within the spreading polymer drop at different time instants for case 2 ($\tau_s \sim \tau_p$) for a drop of radius 0.1 mm. Here we have $\tau_s \approx$ 10.2 ms and $\tau_p \approx$ 66 ms. Velocity profiles within the air have not been shown for the sake of clarity.

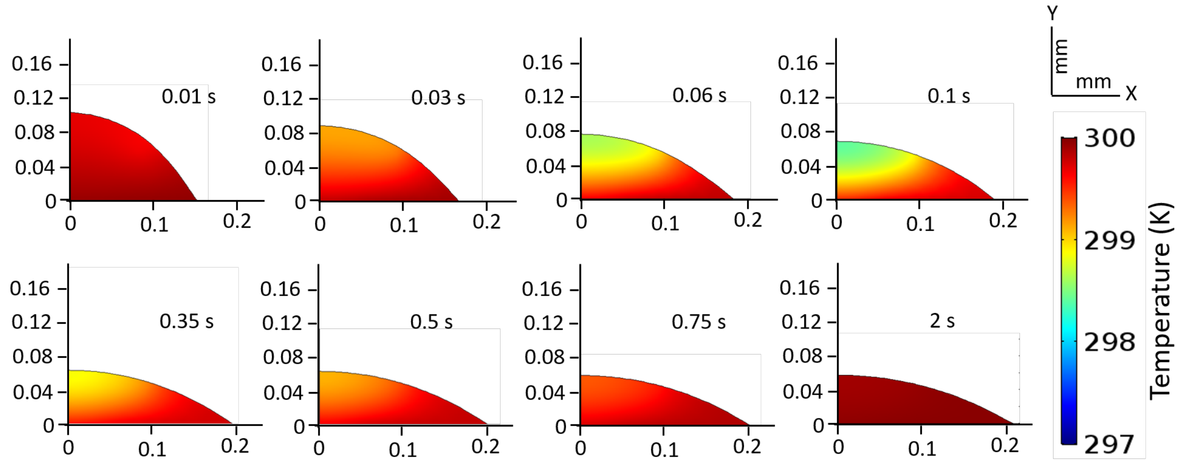

Figure S9: Temperature distribution within the spreading polymer drop at different time instants at different time instants for case 1 ($\tau_s << \tau_p$) for a drop of radius 0.1 mm. Here we have $\tau_s \approx 10.2$ ms and $\tau_p \approx 660$ ms.

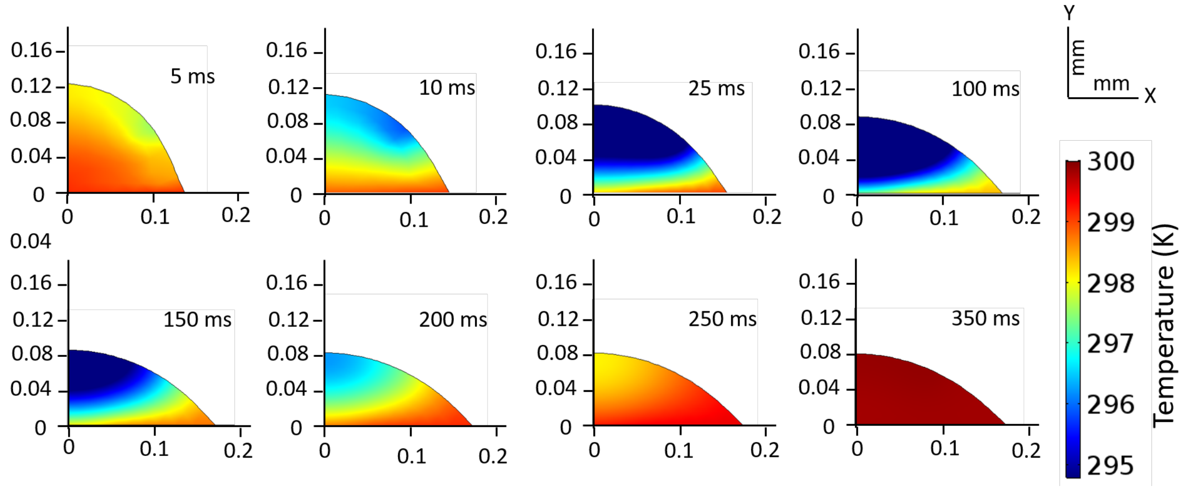

Figure S10: Temperature distribution within the spreading polymer drop at different time instants at different time instants for case 2 (τ_s~τ_p) for a drop of radius 0.1 mm. Here we have $\tau_s \approx$ 10.2 ms and $\tau_p \approx$ 66 ms.

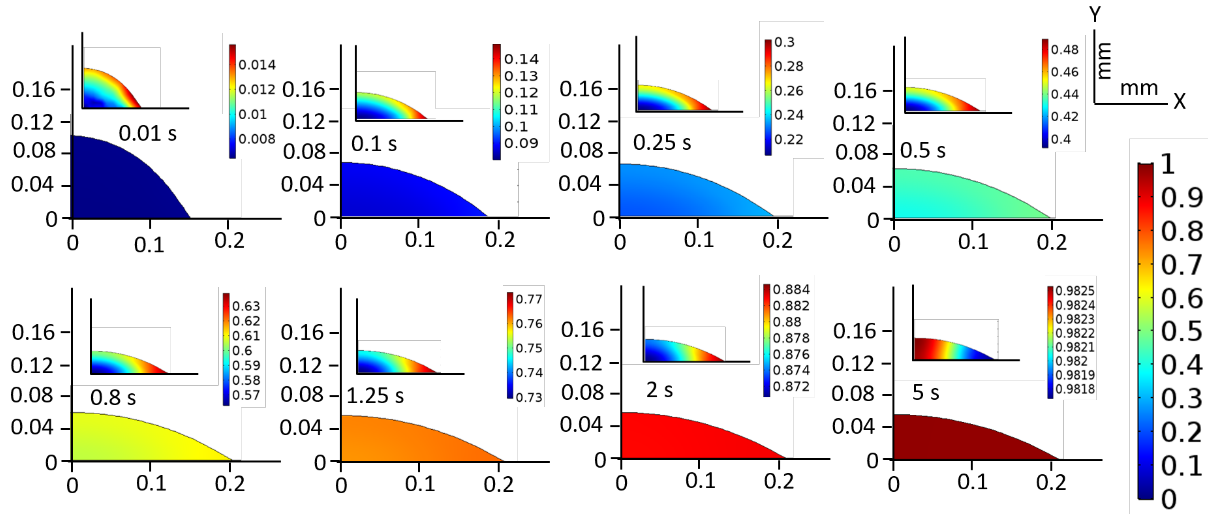

Figure S11: Curing profiles within the spreading polymer drop at different time instants for case 1 (τ_s<<τ_p) for a drop of radius 0.1 mm. Here we have $\tau_s \approx$ 10.2 ms and $\tau_p \approx$ 660 ms.

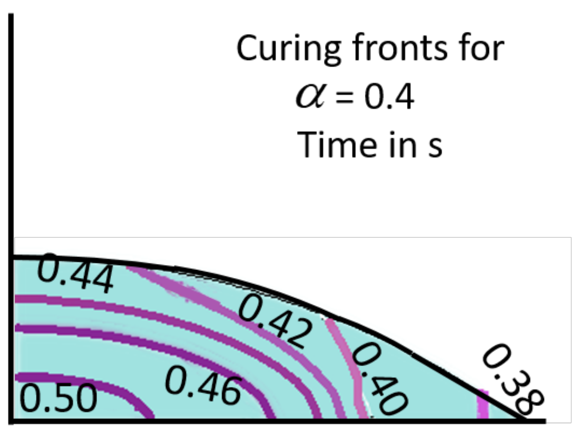

Figure S12: Progression of the curing front (corresponding to α=0.4) within the spreading polymer drop at different time instants for case 1 (τ_s<<τ_p) for a drop of radius 0.1 mm. Here we have $\tau_s \approx$ 10.2 ms and $\tau_p \approx$ 660 ms.

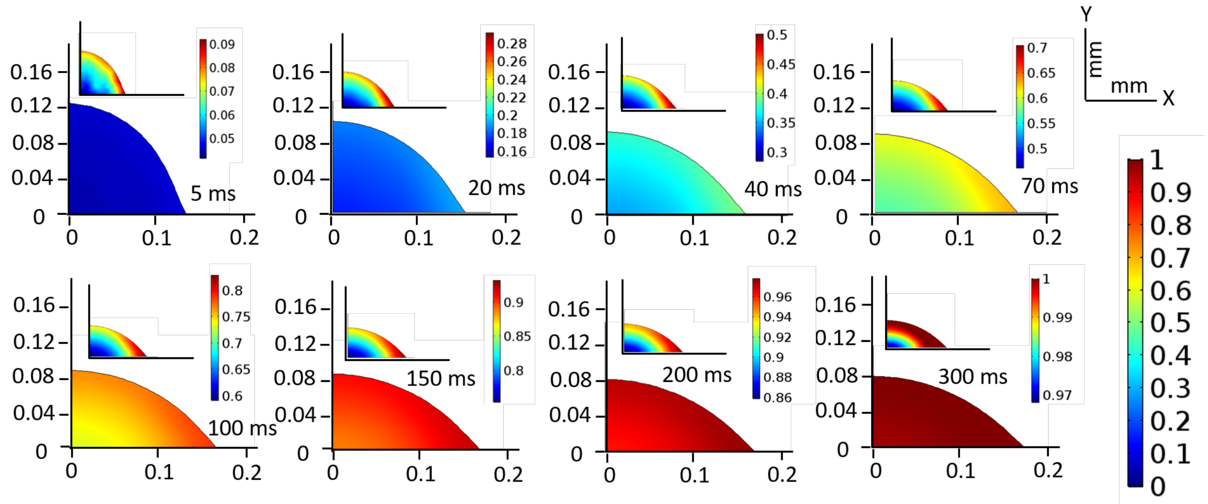

Figure S13: Curing profiles within the spreading polymer drop at different time instants for case 2 (τ_s~τ_p) for a drop of radius 0.1 mm. Here we have $\tau_s \approx 10.2$ ms and $\tau_p \approx 66$ ms. Here we have $\tau_s \approx 10.2$ ms and $\tau_p \approx 66$ ms.

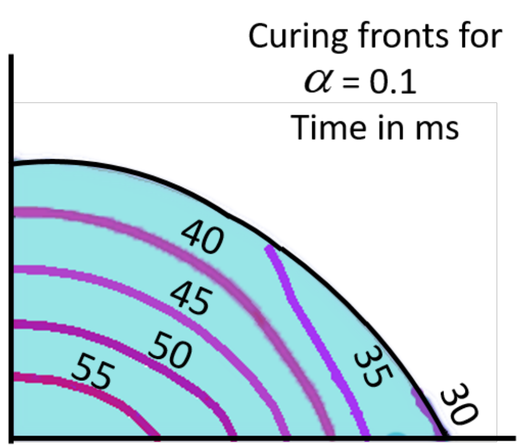

Figure S14: Progression of the curing front (corresponding to α=0.1) within the spreading polymer drop at different time instants for case 2 (τ_s~τ_p) for a drop of radius 0.1 mm. Here we have $\tau_s \approx 10.2$ ms and $\tau_p \approx 66$ ms.

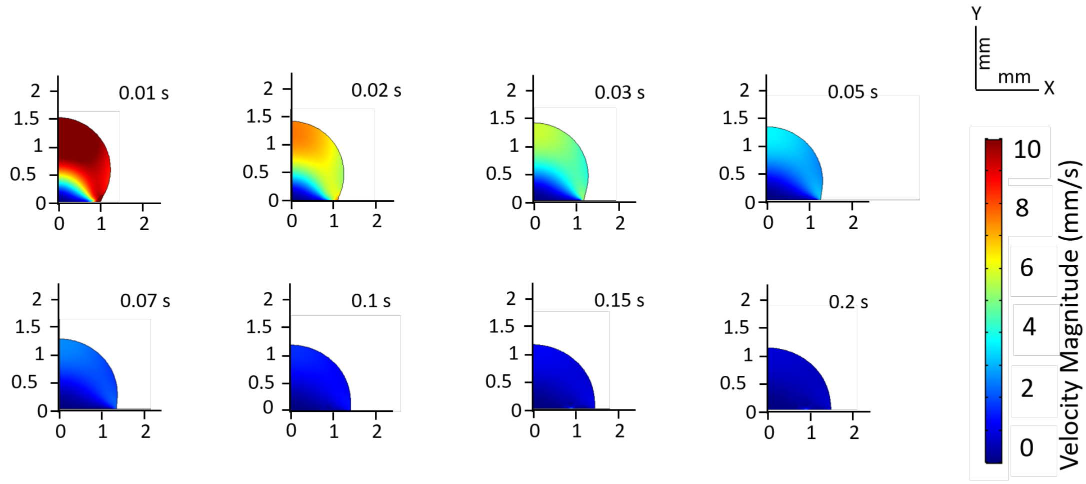

Figure S15: Velocity distribution within the spreading polymer drop at different time instants for case 1 ($\tau_s << \tau_p$) for a drop of radius 1 mm. Here we have $\tau_s \approx$ 107 ms and $\tau_p \approx$ 1200 ms. Velocity profiles within the air have not been shown for the sake of clarity.

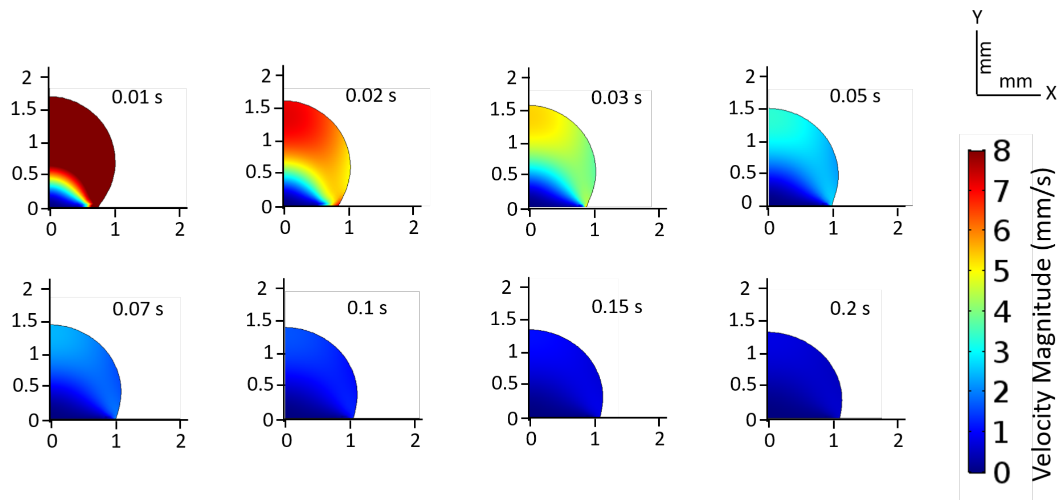

Figure S16: Velocity distribution within the spreading polymer drop at different time instants for case 1 ($\tau_s \sim \tau_p$) for a drop of radius 1 mm. Here we have $\tau_s \approx 107$ ms and $\tau_p \approx 660$ ms. Velocity profiles within the air have not been shown for the sake of clarity.

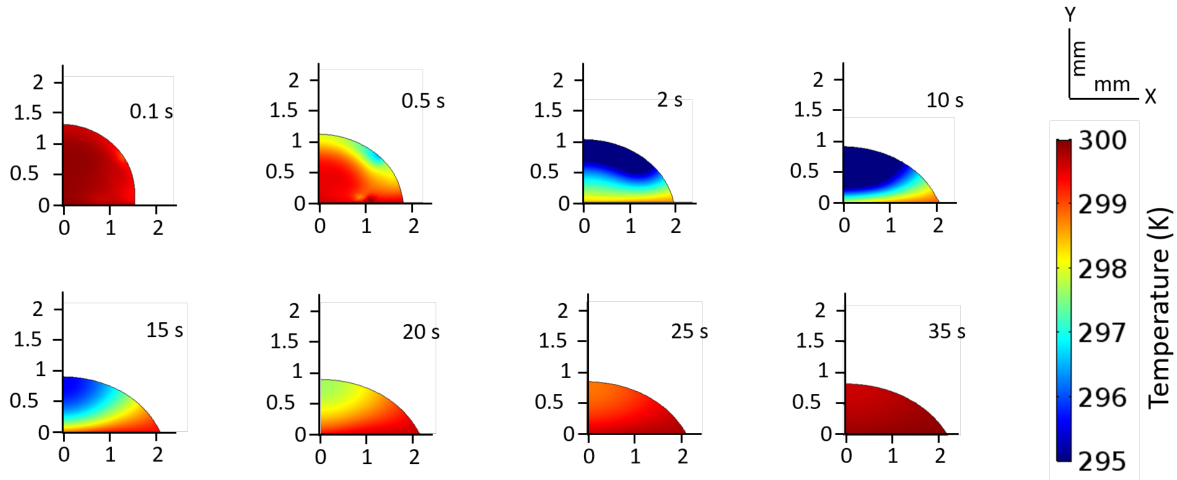

Figure S17: Temperature distribution within the spreading polymer drop at different time instants at different time instants for case 1 (τ_s<<τ_p) for a drop of radius 1 mm. Here we have $\tau_s \approx$ 107 ms and $\tau_p \approx$ 1200 ms.

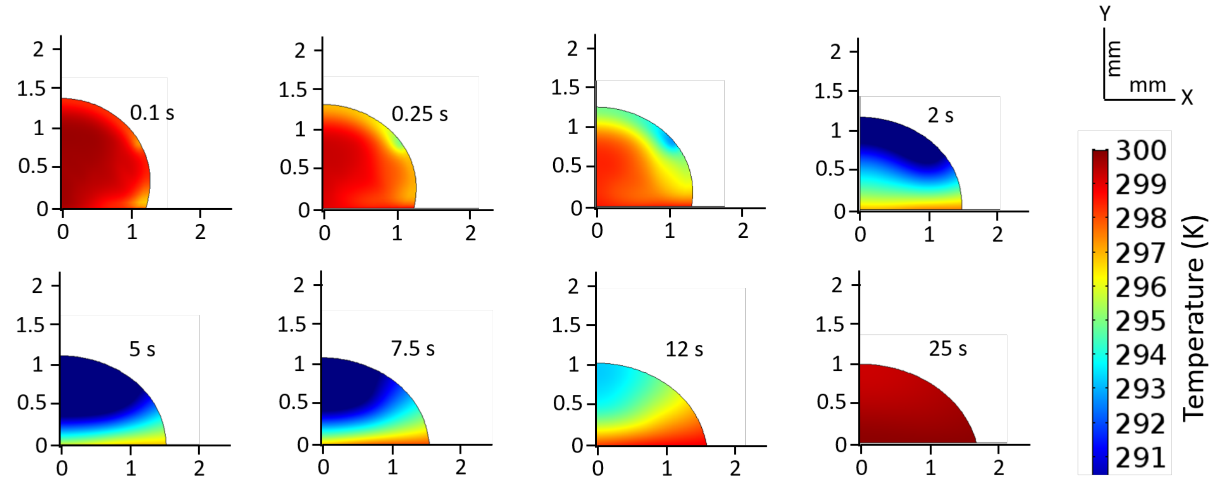

Figure S18: Temperature distribution within the spreading polymer drop at different time instants at different time instants for case 1 (τ_s~τ_p) for a drop of radius 1 mm. Here we have $\tau_s \approx$ 107 ms and $\tau_p \approx$ 660 ms.

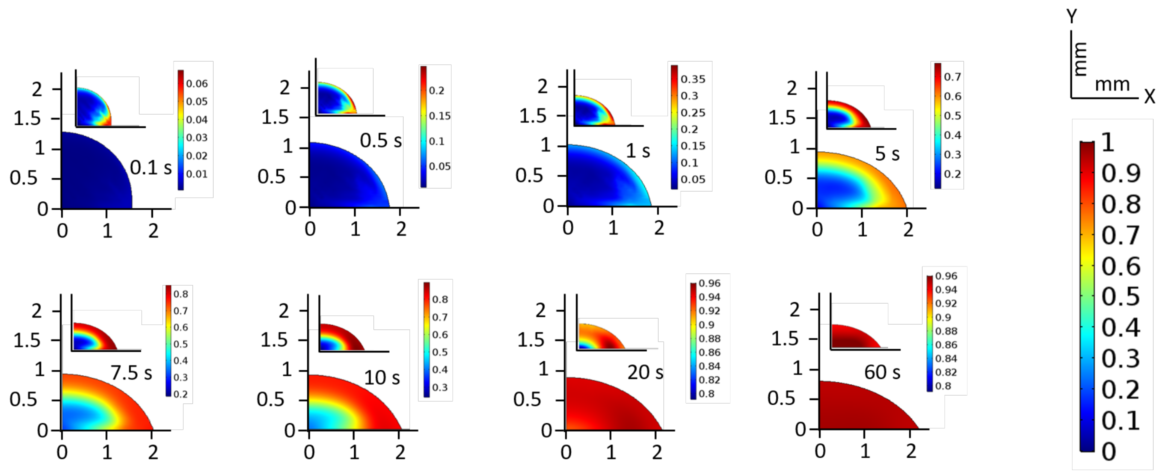

Figure S19: Curing profiles within the spreading polymer drop at different time instants for case 1 (τ_s<<τ_p) for a drop of radius 1 mm. Here we have $\tau_s \approx$ 107 ms and $\tau_p \approx$ 1200 ms.

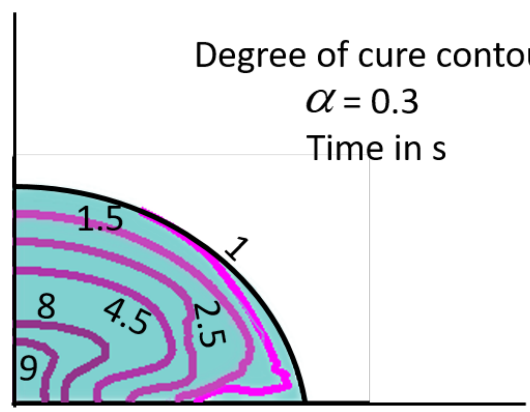

Figure S20: Progression of the curing front (corresponding to α=0.3) within the spreading polymer drop at different time instants for case 1 (τ_s<<τ_p) for a drop of radius 1 mm. Here we have $\tau_s \approx$ 107 ms and $\tau_p \approx$ 1200 ms.

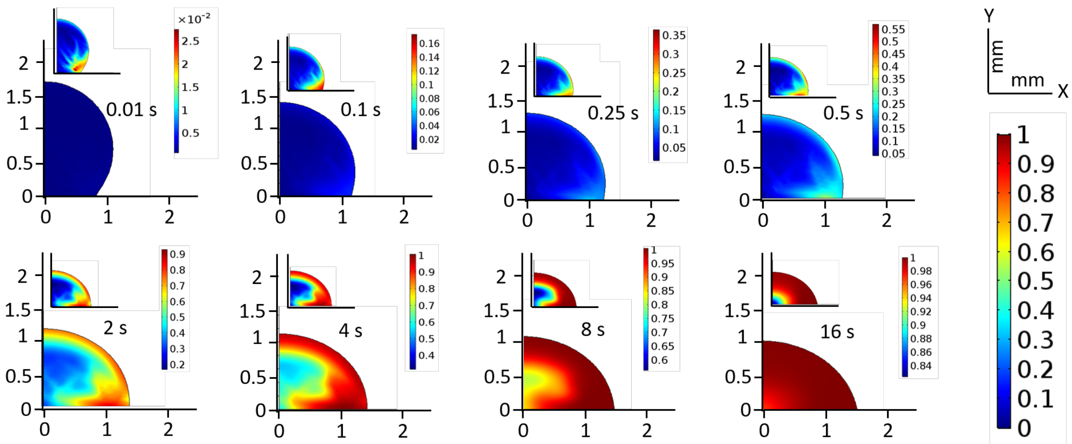

Figure S21: Curing profiles within the spreading polymer drop at different time instants for case 2 ($\tau_s \sim \tau_p$) for a drop of radius 1 mm. Here we have $\tau_s \approx$ 107 ms and $\tau_p \approx$ 660 ms.

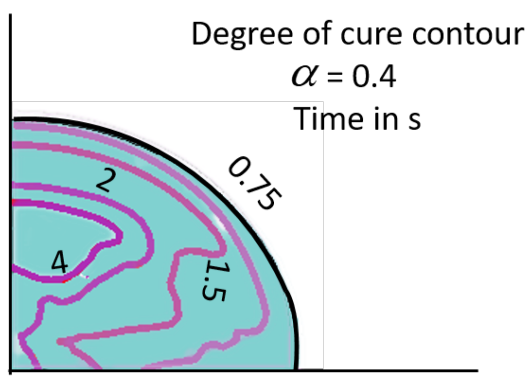

Figure S22: Progression of the curing front (corresponding to α=0.4) within the spreading polymer drop at different time instants for case 2 ($\tau_s \sim \tau_p$) for a drop of radius 1 mm. Here we have $\tau_s \approx$ 107 ms and $\tau_p \approx$ 660 ms.

Table S1: Different Timescales for Drops of Different Sizes

Drop radius (mm)	**τ_c (miliseconds)**	**τ_s (miliseconds)**	**τ_p (miliseconds) for Case 1**	**τ_p (miliseconds) for Case 2**
1	7.21	107	660	1200
0.1	0.228	10.2	66	660
0.01	7.21×10^{-3}	1.1	66	3.3

Table S2: Definition and values of the different parameters used for simulating the the 1-mm drop of 1 wt % of carboxymethylcellulose (CMC) solution (those that are not reported are identical to those reported in Table 1 in the main paper) (Here we don't have the literature for the values that dictate the polymerization process of the CMC drop; therefore, we have chosen these values to be such that ensures that $\tau_s \ll \tau_p$. Under such conditions, the exact values of these parameters don't matter as long as they ensure $\tau_s \ll \tau_p$)

Parameter	Definition	Value	Reference
ρ_m	Density of monomer	1590 [kg/m^3]	Ref. 48 (in the main paper) and using the condition that the Density variation between monomer and polymer is usually less than 10% (Refs. 31,33 in the mian paper)
ρ_p	Density of polymer	1750 [kg/m^3]	
m	Consistency index	7.234	
n	Power law index	0.5088	
σ	Surface tension of the drop/air interface	0.039 [N/m]	
θ	Contact angle	20^0	
k_l	Thermal conductivity of drop	0.603 [W/m/K]	Ref. 49 (in the main paper)
C_{pl}	Heat capacity (at constant pressure) of the drop	4250[J/kg/K]	Ref. 50 (in the main paper)
H_r	Heat of polymerization reaction	-50 [kJ/mol]	
E_p	Activation energy for the propagation reaction	29.7 [kJ/mol]	

E_t	Activation energy for the termination reaction	22.2 [kJ/mol]	Ref. 32 (in the main paper)
A_{p*}	Frequency factor for the propagation reaction for case 1 ($\tau_s << \tau_p$)	2.5×10^9 [L/mol/s]	
A_{t*}	Frequency factor for the termination reaction	10^{11} [L/mol/s]	